DPMJET

Wan Chang

2020.09.10

History of DPMJET

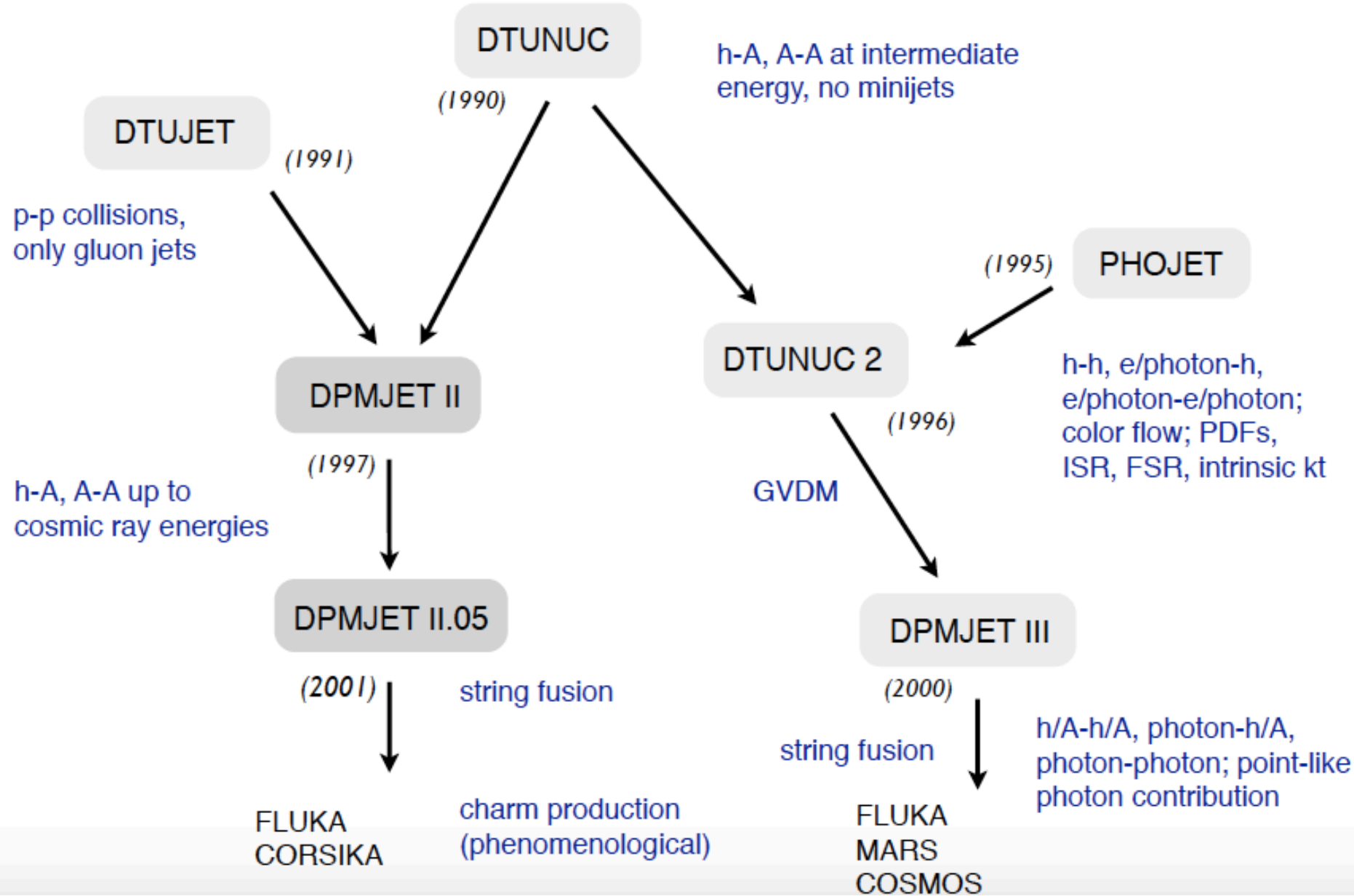

Phys Rev D Part Fields. 1988;37(7):1842-1850

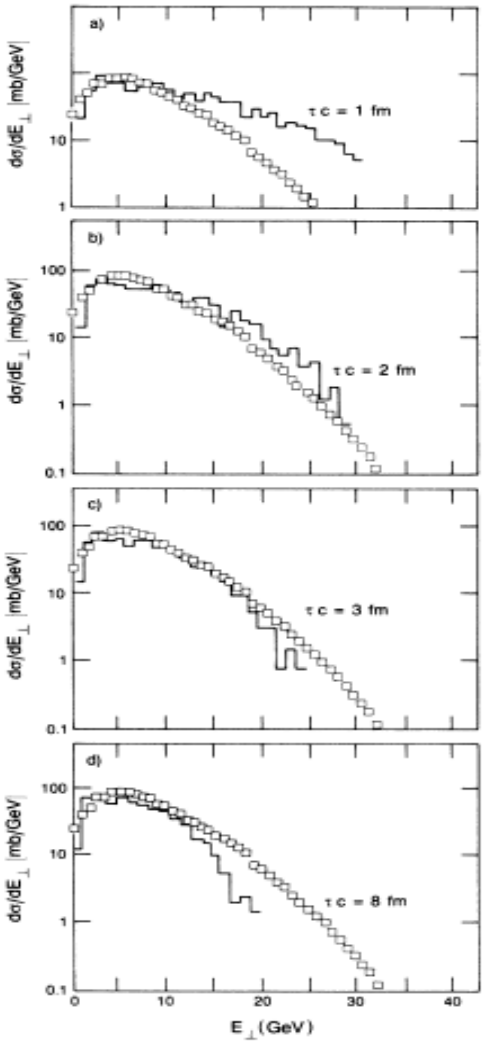

FIG. 7. Transverse-energy distributions $d\sigma/dE_\perp$ for protons interacting on Pb nuclei. The calculations given by histograms are compared to data (points) from the HELIOS Collaboration (Ref. 23) measured in the pseudorapidity range $0.6 \leq \eta \leq 2.4$. The calculation was done with different formation-time parameters τc: (a) $\tau c = 1$ fm, (b) $\tau c = 2$ fm, (c) $\tau c = 3$ fm, (d) $\tau c = 8$ fm.

The transverse-energy distribution $d\sigma/dE_\perp$ with different formation-time parameter for p-Pb collisions at 200 GeV/c of incident proton momentum:

a) $\tau c = 1fm$ b) $\tau c = 2fm$

c) $\tau c = 3fm$ d) $\tau c = 8fm$

The data are taken in the pseudorapidity range 0.6 <eta<2.4. In this rapidity range the intranuclear cascade corrections to the model are significant. The best agreement for $\tau c = 2 - 3fm$

HELIOS (NA34) Collaboration at the CERN Super Proton Synchrotron

Phys Rev D Part Fields. 1988;37(7):1842-1850

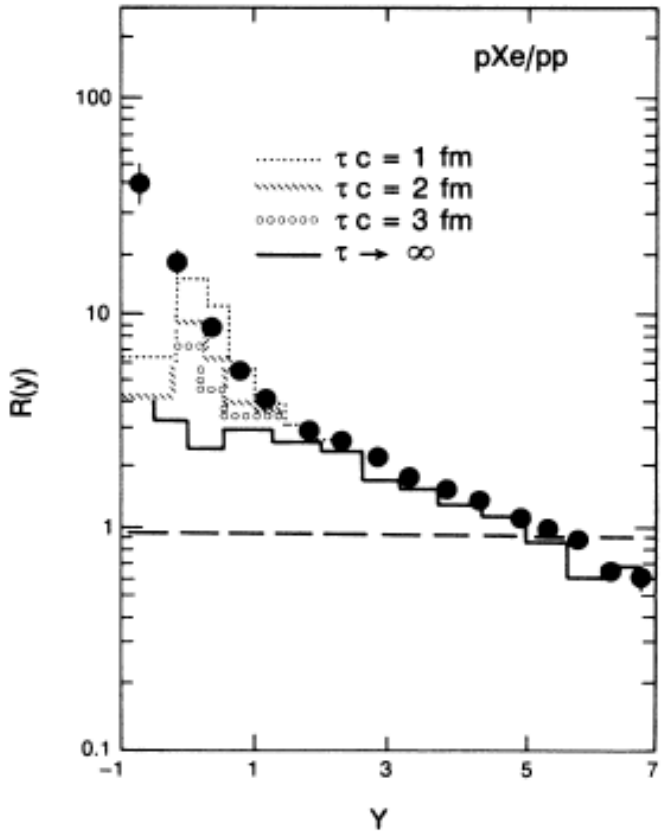

FIG. 6. Rapidity ratios $R(y)=[dN/dy(p\text{-Xe})]/[dN/dy(p\text{-p})]$ for all charged particles at proton energies in the laboratory frame $p_{lab}=200$ GeV/c. The Monte Carlo results represented by histograms are compared to data from Ref. 22. The lowest histogram corresponding to $\tau\to\infty$ was already calculated in Ref. 8.

rapidity ratio $\left(R(y)=\frac{dN^{p-A}}{dy}/\frac{dN^{p-p}}{dy}\right)$ calculated with different τc parameters again with the data ($p_p = 200GeV/c$)

A disagreement is found at low rapidity in the target rest frame. Above rapidity y =2 the agreement of the model and the measured rapidity distributions and rapidity ratios was rather good. At rapidity below y =2 the measured rapidity ratios were bigger than the calculated ones.

The optimum formation-time parameter in this comparison is $\tau c = 1 - 2fm$

Z. Phys. C - Particles and Fields 52, 643-653 (1991)

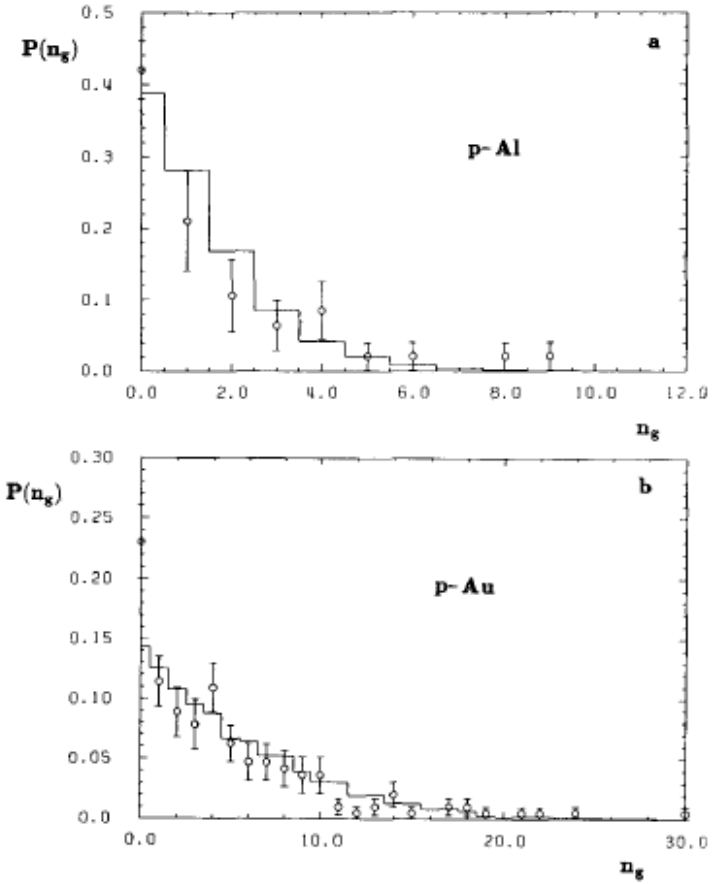

Fig. 3. Multiplicity distributions of grey particles produced in **a** p–Al and **b** p–Au interactions at 360 GeV. In accordance with the data analysis [21], positively charged particles with momenta corresponding to ionization losses larger than 1.3 times the minimum ionization were defined to be grey tracks for this comparison

Multiplicity distributions of grey particles produced in a) p-Al and b) p-Au interactions at 360GeV

positively charged particles with momenta corresponding to ionization losses larger than 1.3 times the minimum ionization were defined to be grey tracks for this comparison.

The calculated average numbers of grey tracks, n_g = 1.3 and 5.3 for p-Al and p-Au interactions, respectively, are to be compared with the experimental numbers of 1.9 ± 0.5 and 4.6 ± 0.4.

DPMJET new features

arXiv:hep-ph/9911213

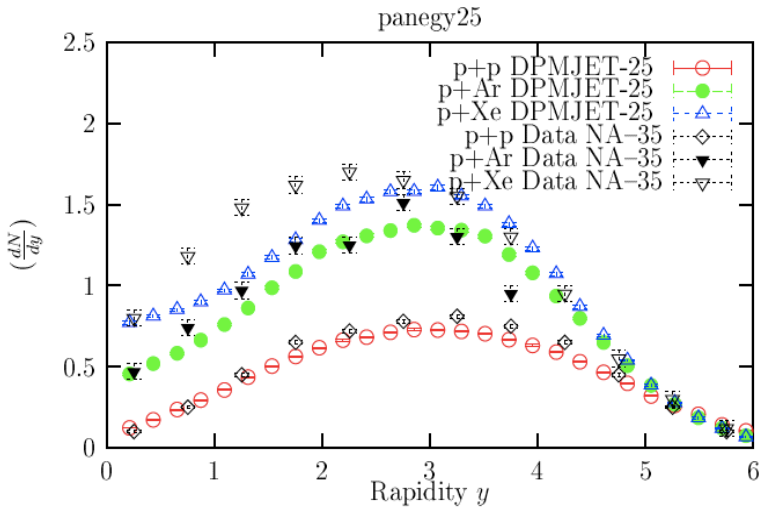

the comparison is the rapidity distribution of negatively charged hadrons in p–p, p-Ar and p–Xe collisions at 200 GeV.

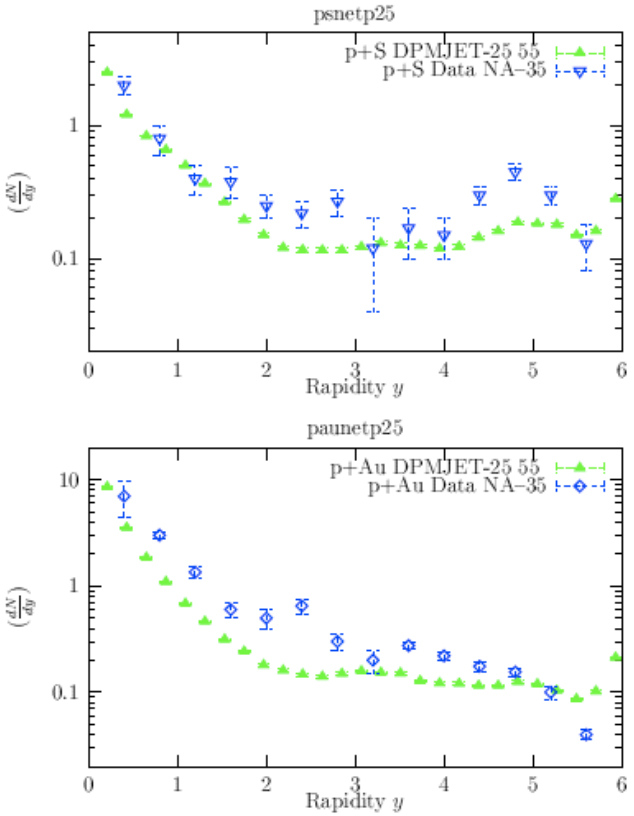

FIG. 24. **(a)** Net proton $(p-\bar{p})$ rapidity distribution in p–S collisions. The DPMJET–II.5 results are compared with data [49]. **(b)** Net proton $(p-\bar{p})$ rapidity distribution in p–Au collisions. The DPMJET–II.5 results are compared with data [49].

NA35: NA35 experiment at the CERN SPS Experiment NA35 at the CERN SPS studies collisions of p, d, O and S projectiles of 200 GeV per nucleon incident energy (√sNN=19.4 GeV) with nuclear targets.

Net proton $(p-\bar{p})$ rapidity distribution in p–S collisions (a) and p-Au collisions (b).

Z. Phys. C 70, 413–426 (1996)

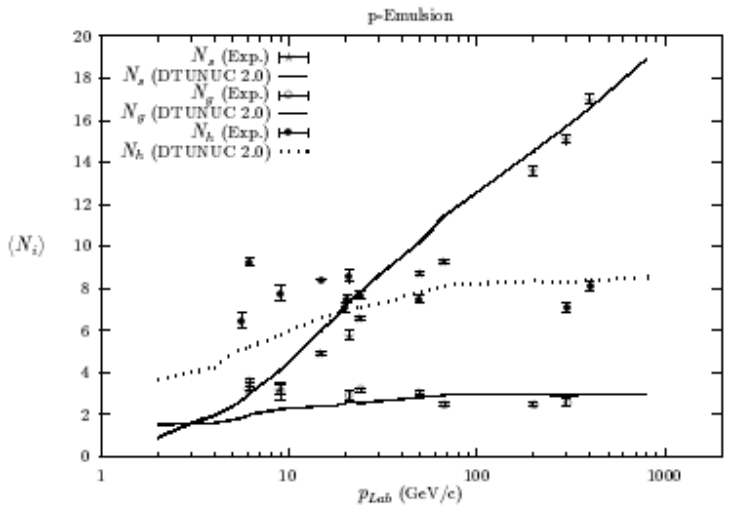

Fig. 4. Mean multiplicities of shower, grey, and heavy particles in collisions of protons with emulsion nuclei. Data from various experiments [40] (points) are compared to results of the model (lines)

the emulsion consisting of 28.8% of light nuclei and of 71.4% of heavy nuclei

grey particles: singly charged particles with a Lorentz-β value $0.23<\beta<0.7$
black particles: singly and multiply charged particles with $\beta < 0.23$.
shower particles: $\beta > 0.7$
heavy particles: grey + black

Whereas the average number of shower particles is increasing throughout the whole energy range and get an increasing multiplicity of grey and black particles up to about 40 GeV/c which turns into an almost constant behaviour for higher energies. Within the model, this constant behaviour is due to limiting fragmentation in each hadron-nucleon interaction together with a constant formation zone intranuclear cascade and inelastic hadron-nucleus cross sections depending only weakly on the projectile energy.

For momenta above about 20 GeV/c the model agrees well with measured multiplicities, whereas at low energies our results seem to depart from the experiments. / From this comparison it is difficult to draw conclusions about the applicability of the model of slow particle production to energies below 10-20 GeV and to modifications within the model which could be necessary to reproduce the observed threshold behaviour.

Z. Phys. C 70, 413–426 (1996)

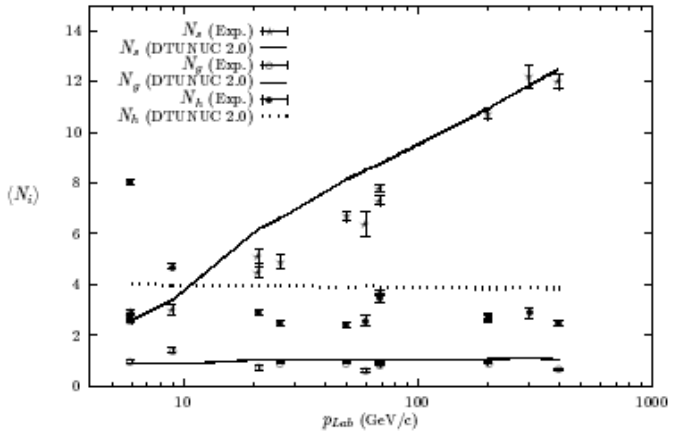

a)

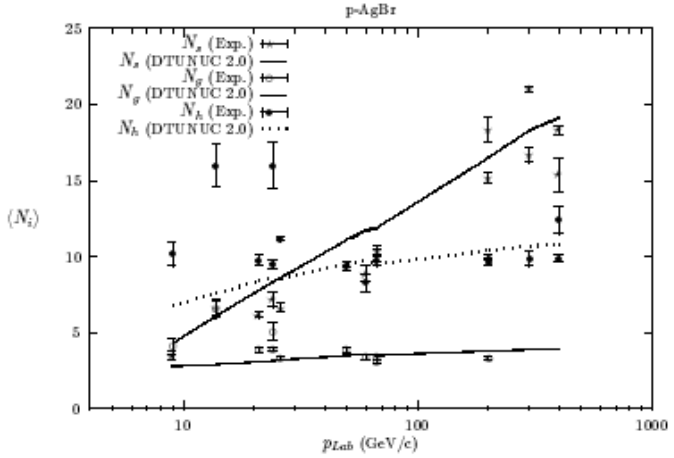

b)

Fig. 5. Mean multiplicities of shower, grey, and heavy particles in collisions of protons with emulsion nuclei are shown for the component consisting of light nuclei (C,N,O) **(a)** and the heavy component (Ag, Br) **(b)**. Data from various experiments [40] (points) are compared to results of the model (lines)

the mean grey, black, and heavy particle multiplicities for the light component(C, N, O).

It seems, that the model overestimates the black particle multiplicity which could be due to the absence of the treatment of the nuclear skin in the nuclear potential, i.e. by underestimating the low part of the excitation energy distribution.

the mean grey, black, and heavy particle multiplicities for the heavy component (Ag, Br).

An average value of one grey particle per interaction agrees well with the experimental results. The model reproduces the measured multiplicities of slow particles in interactions of protons with nuclei of the heavy component down to a proton momentum of about 20 GeV/c.

Z. Phys. C 70, 413–426 (1996)

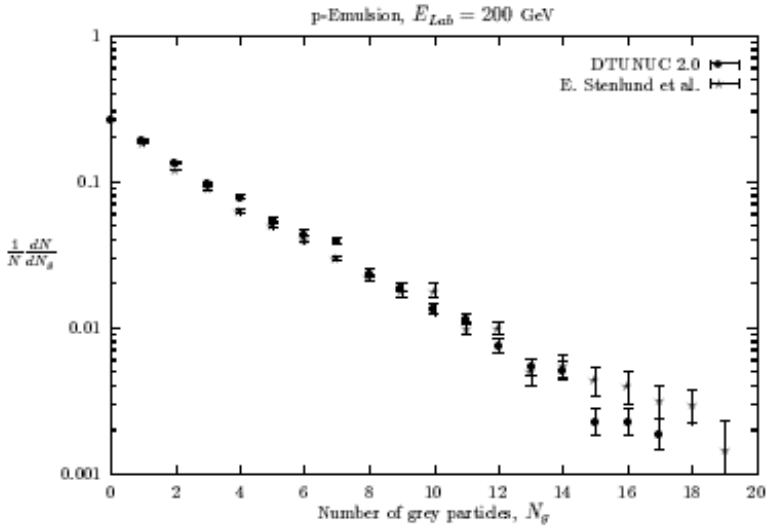

a)

Grey particles

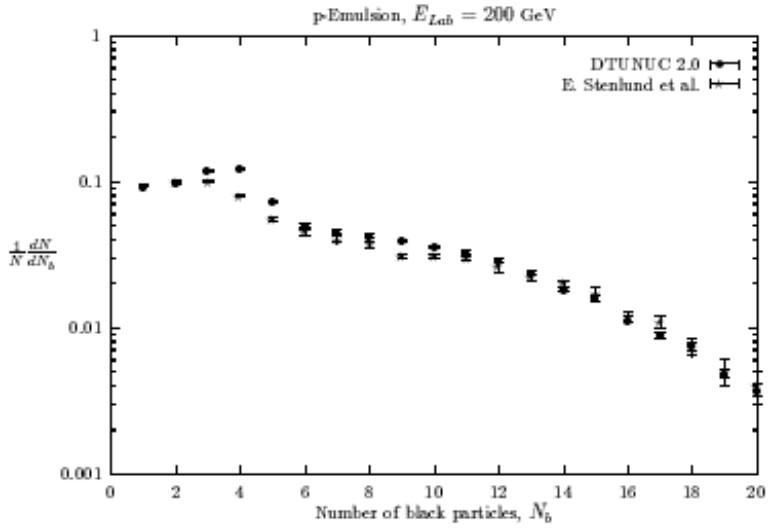

a)

Black particles

the grey and black particle multiplicity distributions normalized to unity for proton-emulsion interactions at 200 GeV.

As the comparisons show, model is able to reproduce the data on slow particle multiplicities very well. The grey particle multiplicity distribution for proton projectiles slightly underestimates the measured distribution at high multiplicities which,however, might be not very conclusive since the uncertainties within the experimental data are rather big in this region.

Z. Phys. C 70, 413–426 (1996)

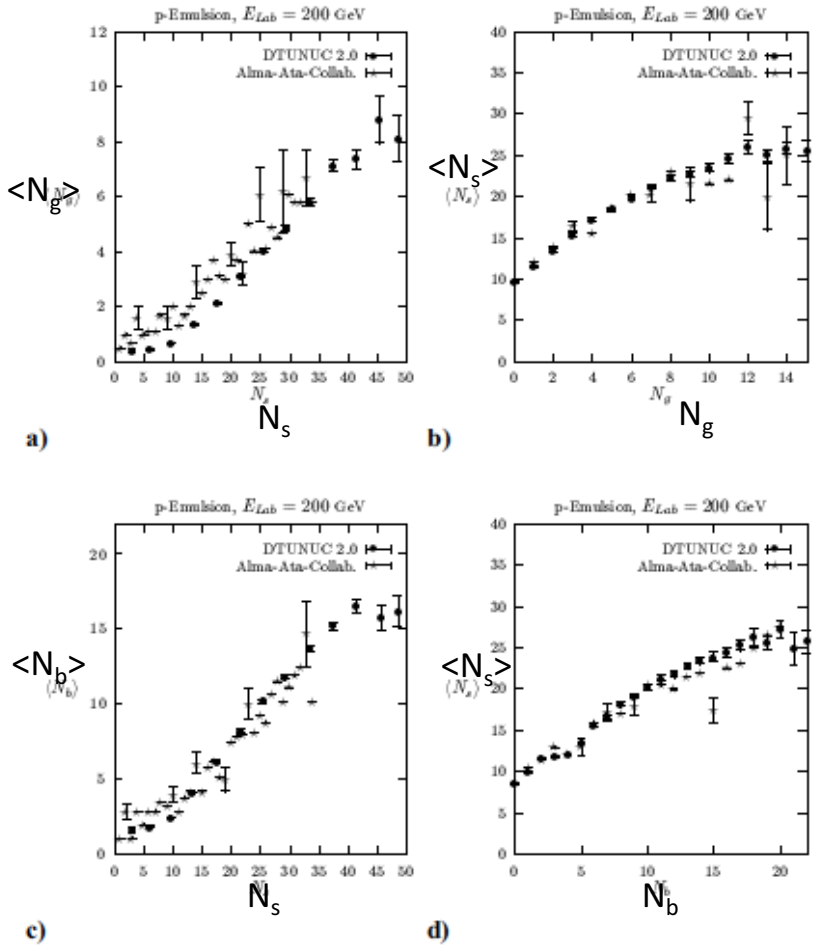

Fig. 8. The correlations between grey (N_g) and shower (N_s) particle multiplicities **(a,b)** and black (N_b) and shower particle multiplicities **(c,d)** in interactions of protons with emulsion nuclei are compared to experimental results [39]

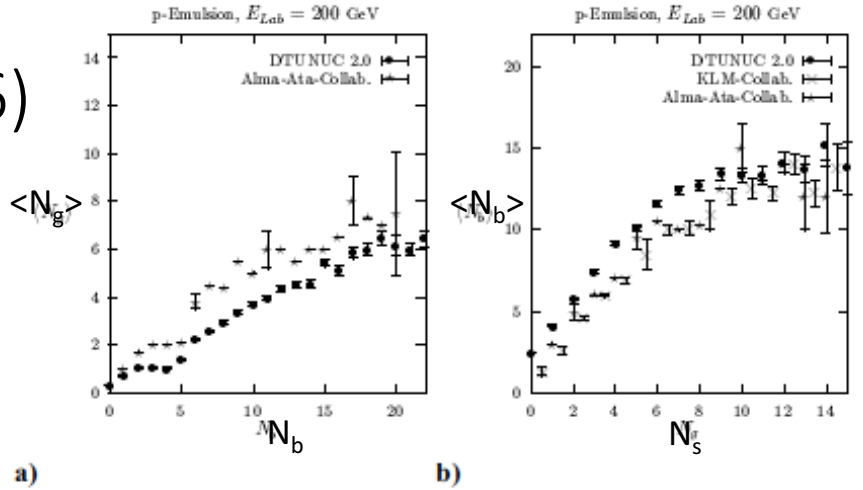

Fig. 9. The correlations between grey (N_g) and black (N_b) particle multiplicities in interactions of protons with emulsion nuclei are compared to experimental results [39, 42]

Apart from the correlation between grey and black particles, where we obtain slightly more black particles for a fixed number of grey particles than seen in the experiments, the calculations are in good agreement with the data within their uncertainties.

Z. Phys. C 70, 413–426 (1996)

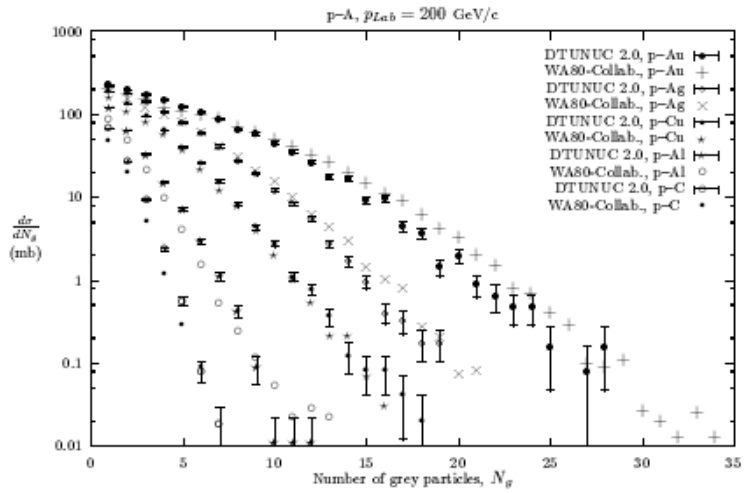

a)

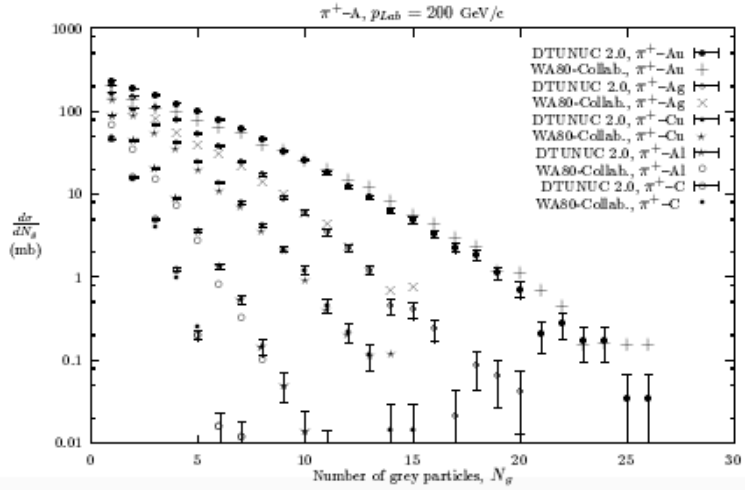

b)

grey particle multiplicity distributions in interactions of protons a) and pions b) with different target nuclei at 200 GeV/c

grey particles are defined as singly charged particles with a kinetic energy between 30 MeV and 400 MeV emitted in the target
rapidity region ($-1.7 < \eta < 1.3$).

All calculated distributions are normalized to the Glauber cross sections of the corresponding interactions. For the two light nuclei (C,Al), the model distributions are consistently broader than the experimental distributions, whereas for heavier targets they agree well in shape and absolute normalization with the data.

Z. Phys. C Particles and Fields 43, 439-446 (1989)

Energy: 200GeV/Ap

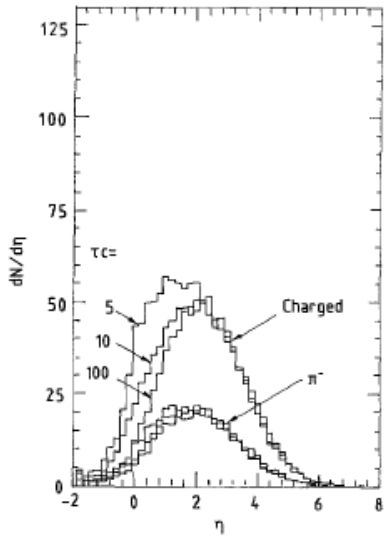

Fig. 2. Pseudorapidity distributions for charged secondaries and π^- mesons created in O–Au collisions as calculated in the dual parton model with three different formation zones, $\tau_0 c = 100$, 10 and 5 fm

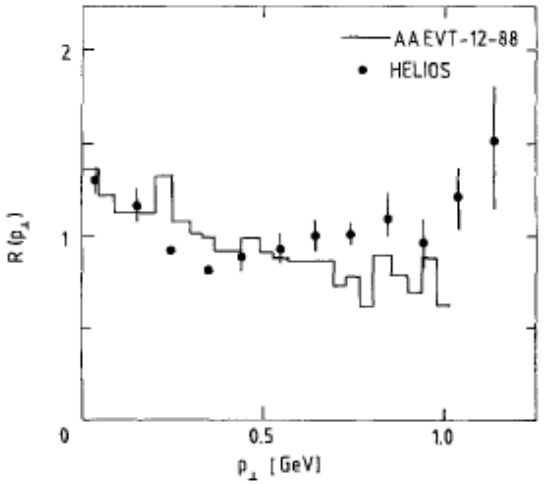

Fig. 3. The ratio of the inclusive transverse momentum distribution in p–Au collisions as calculated in the model with formation zone cascade ($\tau_0 c = 5$ fm) to the model without formation zone cascade. This ratio is compared with the ratio of the measured transverse momentum distributions in O–Au collisions to the one in p–p collisions [15]

In Fig. 2 present pseudorapidity distributions of charged particles in central O-Au collisions for the three formation zones $c\tau_0$ = 100, 10 and 5 fm. The distributions at large pseudorapidity in the laboratory (target) frame is hardly changed by the changing formation zone. The increase of the particle production with decreasing formation zone comes mainly at laboratory below η= 2. At η around 0 to 1 the production might increase by as much as a factor 2 to 3. It seems that rapidity or pseudorapidity distributions in the region below y or η = 2 offer the best possibility to determine the formation zone from experimental data.

The formation zone cascade also changes the transverse momentum distribution. The hadrons created by secondary particles interacting in the target nucleus have in general smaller transverse momenta than the interacting particles.

This can be seen in Fig. 3, where plot the ratio of the transverse momentum distribution in p-Au collisions with the formation zone $c\tau_0$ = 5fm to the distribution calculated with the formation zone $c\tau_0$ = 100, where no formation zone cascade occurs. The comparison suggests that the low Pt enhancement in the data might be due to the formation zone cascade.

hep-ph/9611379

Target experiments

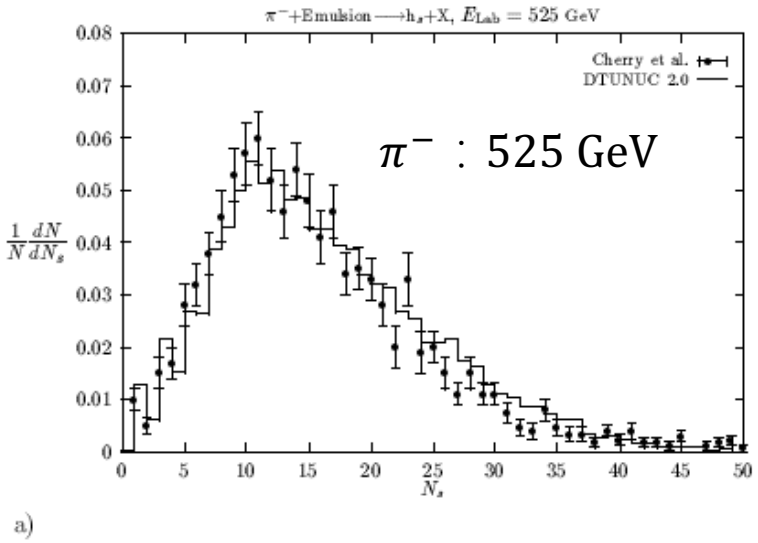

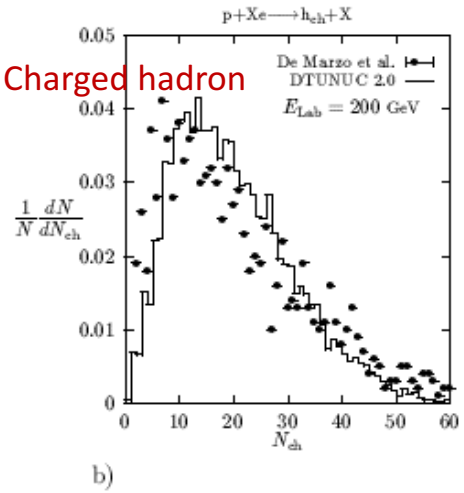

Charged hadron

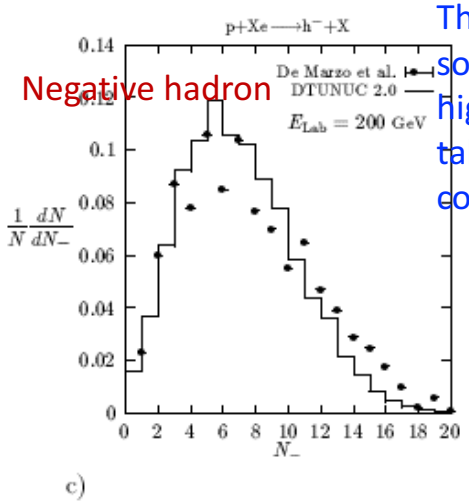

Negative hadron

a): shower particles results for interactions of negatively charged pions in nuclear emulsions at 525 GeV. The agreement is satisfactory .

b) and c): the multiplicity distributions of charged and of negatively charged particles in proton-xenon interactions at 200 GeV

The calculated distribution in b) seems to be peaked at somewhat higher multiplicities with a stronger decrease towards higher multiplicities than the measured distribution. However, taking the statistical uncertainties within the measurements into consideration these differences might be not significant.

Fig.5

hep-ph/9611379

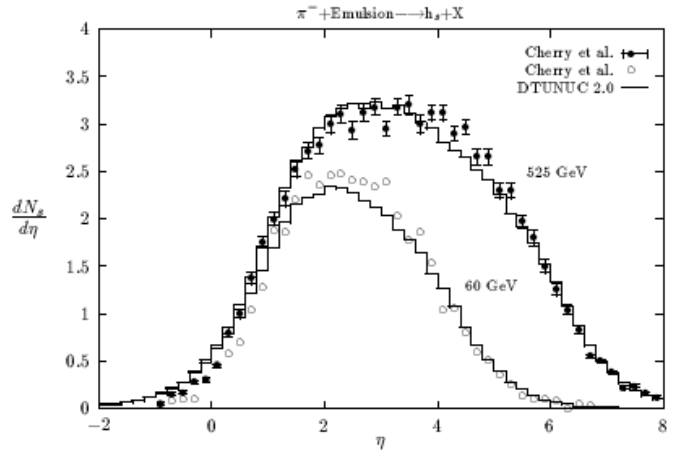

Target experiments

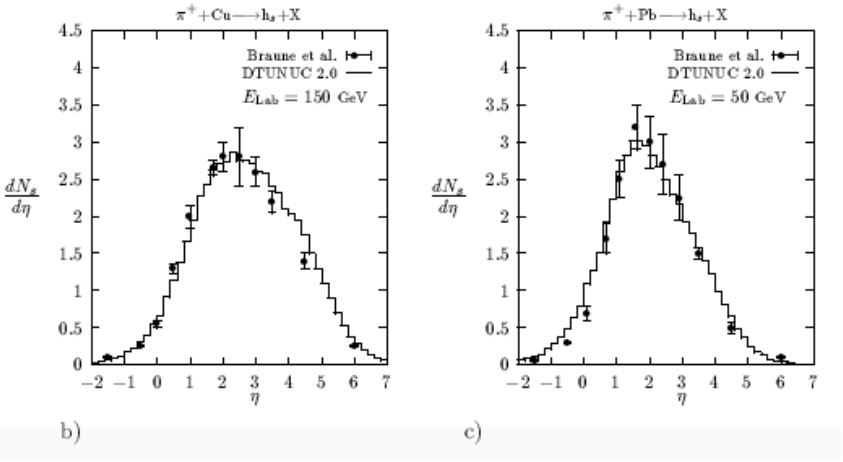

Fig.6

Pseudorapidity distributions of shower particles in pion-nucleus interactions.

a): pion-emulsion interactions at E_{Lab} = 60 GeV and 525 GeV

b): pion-copper interactions at 150 GeV

c): pion-lead interactions at 50 GeV

Again, the results of the measurements are well reproduced within our model.

hep-ph/9611379

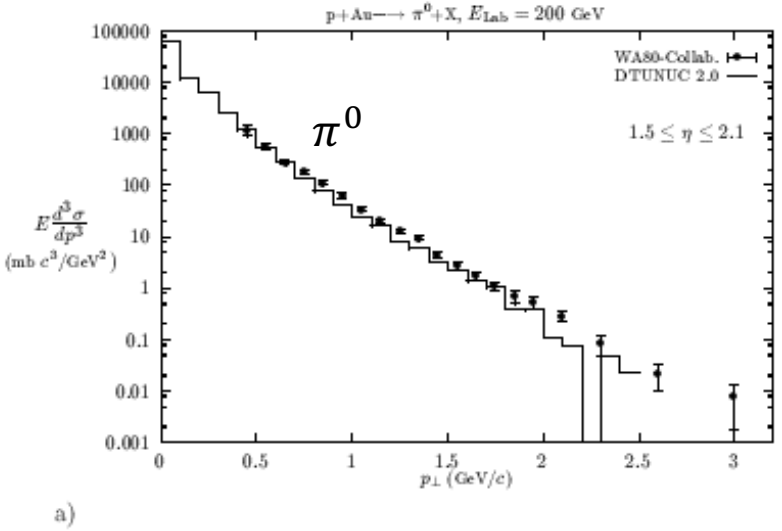

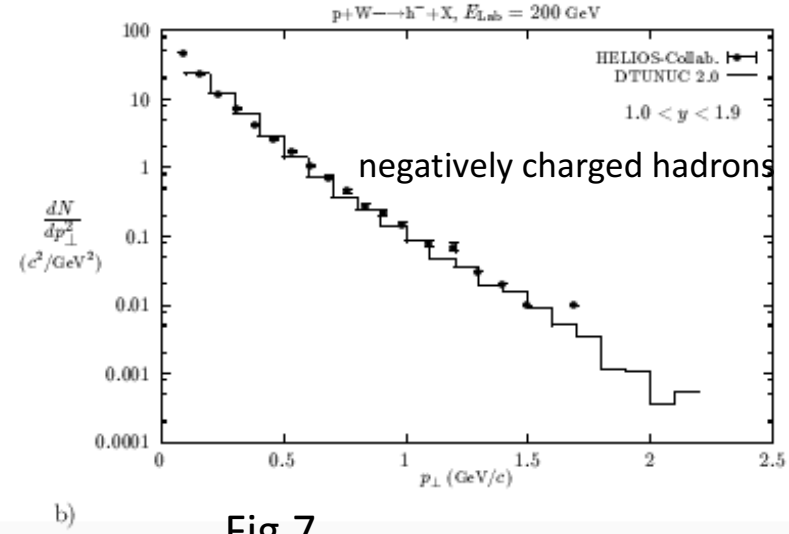

Fig.7

a): The invariant π^0 cross section as a function of the transverse momentum in proton-gold collisions at 200 GeV. (pseudorapidity range $1.5 < \eta \ 2.1$)

b): the transverse momentum distribution is shown for negatively charged hadrons from proton-tungsten collisions at 200 GeV in the rapidity range between 1.0 and 1.9.

In both case we observe a reasonable agreement between experimental data and calculation.

hep-ph/9611379

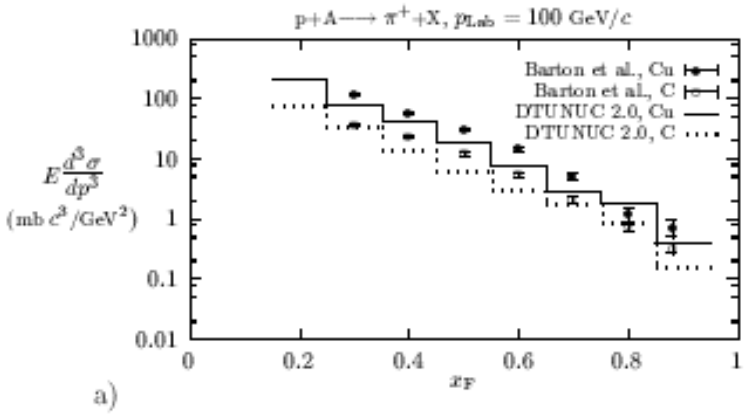

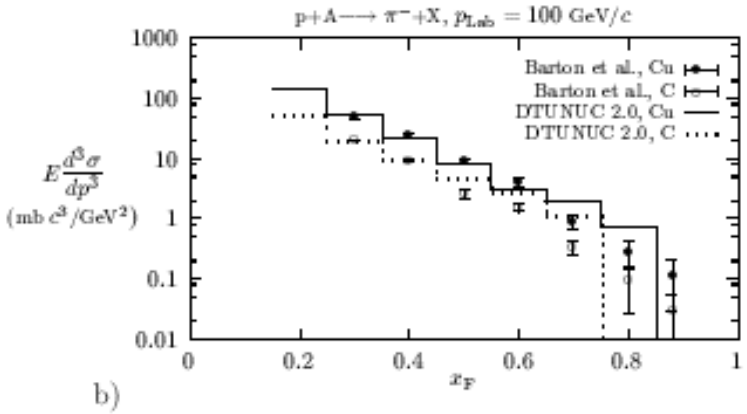

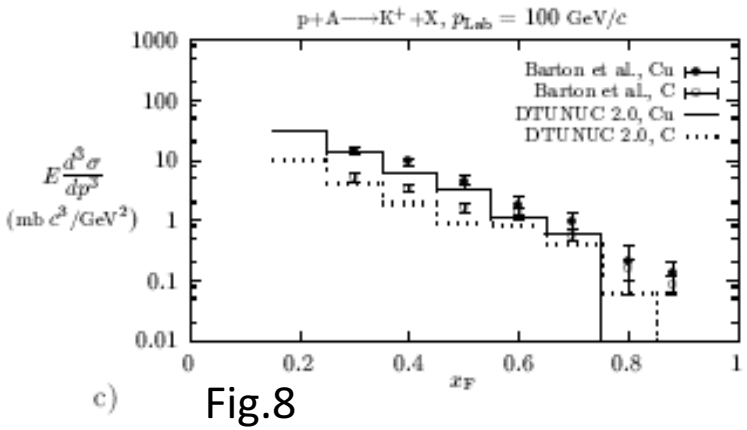

Fig.8

Feynman-xF distributions of positively (a) and negatively charged pions (b) and of positively charged kaons (c) in interactions of protons with copper and carbon at 100 GeV are shown for xF >0.2 (histograms). The calculated distributions are restricted to hadrons with transverse momenta are between 0.25 GeV/c and 0.35 GeV/c.

The measured cross sections include only particles with transverse momenta $p_\perp$ = 0.3 GeV/c. From the calculated nal state, pions and kaons with 0.25 < $p_\perp$ < 0.35 GeV/c were taken into consideration. Discrepancies seem to exist within the slopes of the pion-cross sections: from calculations we obtain about equal slopes for positive and negative pions whereas the measurements indicate a larger slope for negative as compared to positive pions.

The kaon cross sections are at large xF slightly underestimated by the calculations.

hep-ph/9611379

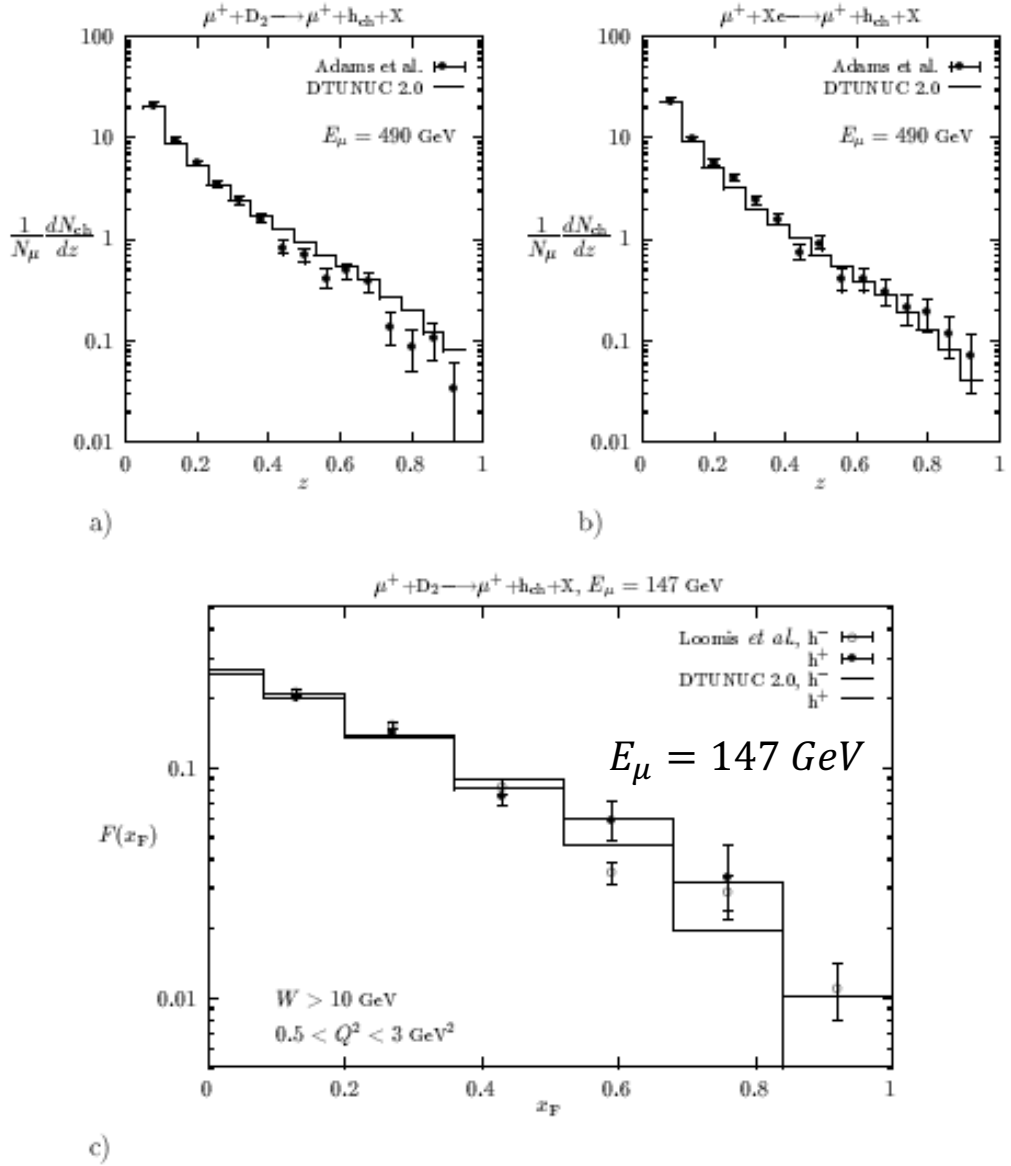

Fig.16

Distributions of charged hadrons from muon-deuterium and muon-xenon interactions at 490 GeV were studied as function of $z = E/\nu$ (E and ν being the secondary hadron energy and the photon energy in the target rest frame, resp.)

Energy- (z-) distributions of charged hadrons from muon-deuterium (a) and muon-xenon interactions (b) at 490 GeV .
Corresponding to the experimental cuts applied to the data the MC-results are restricted to xBj < 0.005, Q2 < 1 GeV^2, and nu > 100 GeV.

In c) model results for Feynman-xF distributions of charged hadrons from muon-deuterium interactions at E_{Lab} = 147 GeV are compared to data. Here the photon virtualities are restricted to the range $0.5<Q^2<3$ GeV and the photon nucleon c.m. energies to W>10 GeV.

We find a good agreement in the whole z range.

- Backup

History of DPMJET

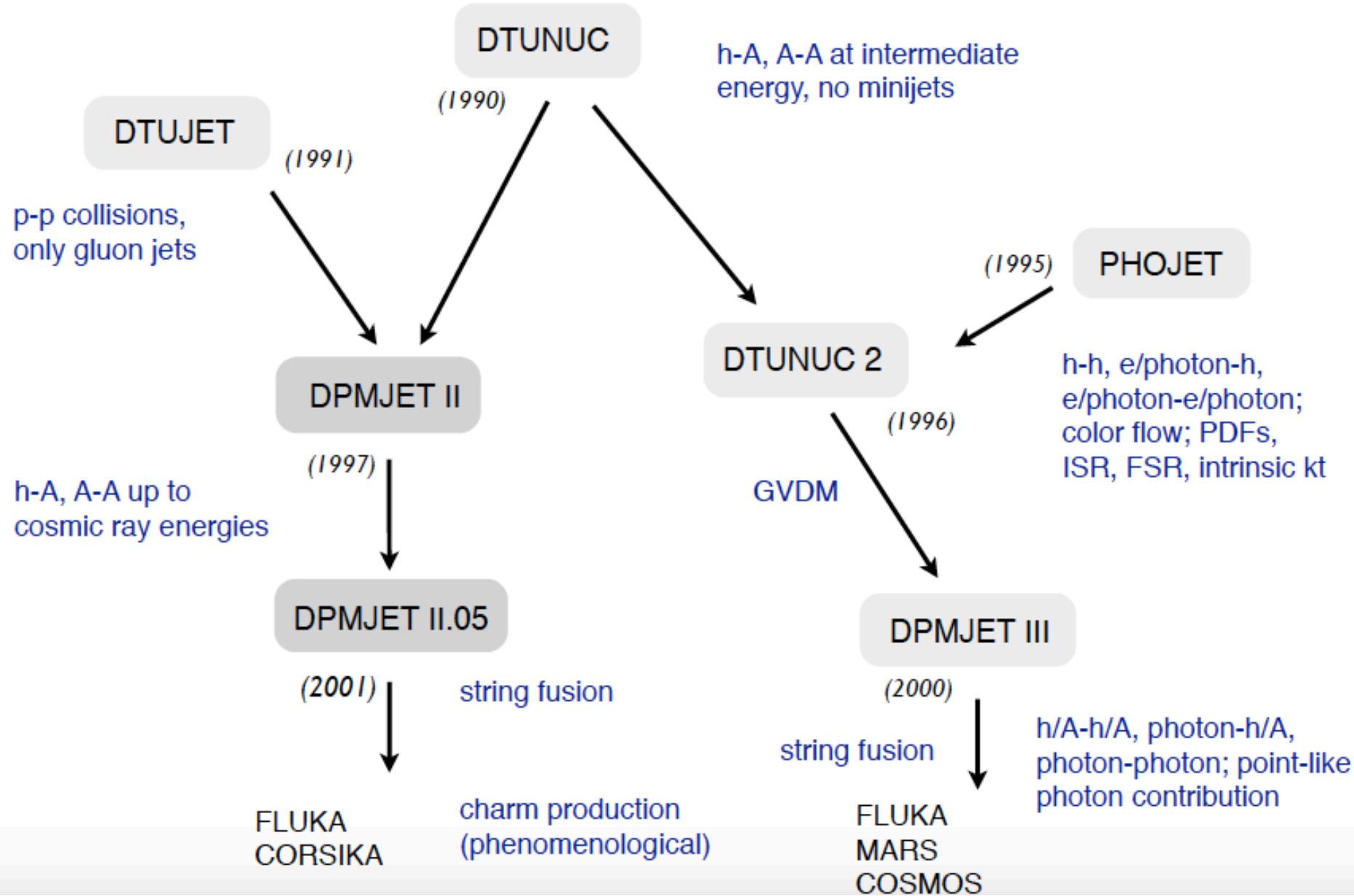

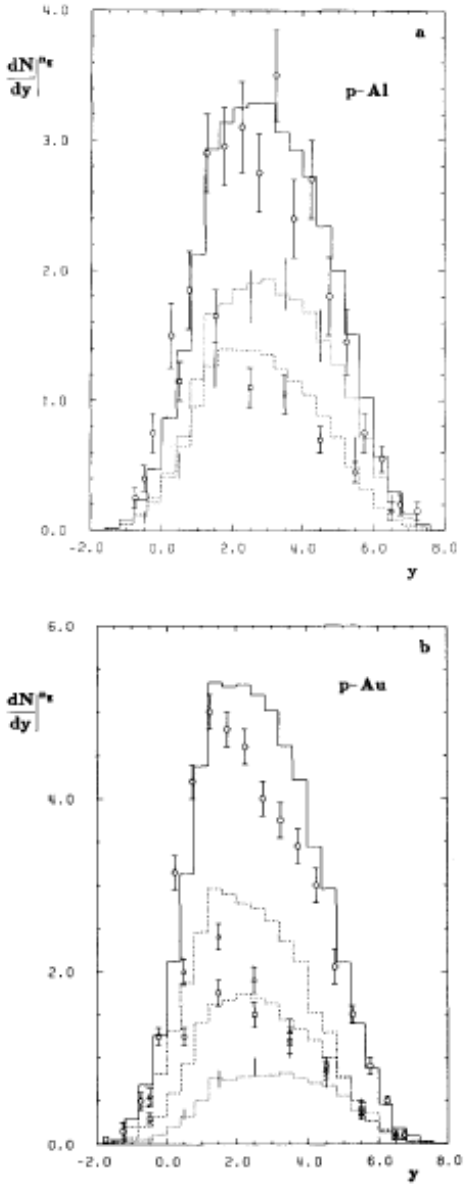

Fig. 4. Rapidity distributions of charged particles in **a** p–Al and **b** p–Au interactions at 360 GeV. The events are classified according to the number of grey particles (as defined in Fig. 3): **a** p–Al: $0 \leq n_g \leq 1$ – dashed line, $n_g \geq 2$ – dotted line, all n_g – full line; **b** p–Au: $0 \leq n_g \leq 1$ – dashed line, $2 \leq n_g \leq 5$ – dotted line, $n_g \geq 6$ – dashed-dotted line; all n_g – full line. The data are taken from [21]; grey prongs are not included in the distributions presented

Z. Phys. C - Particles and Fields 52, 643-653 (1991)

Rapidity distributions of charged particles in a) p-A1 and b) p-Au interactions at 360GeV. The events are classified according to the number of grey particles: a) pAl: $0 \leq n_g \leq 1$ - dashed line, $n_g \geq 2$ dotted line, all n_g - full line; b) pAu: $0 \leq n_g \leq 1$ - dashedline, $2 \leq n_g \leq 5$ - dotted line, $n_g \geq 6$ dashed dotted line; all n_g - full line.

Phys Rev D Part Fields. 1988;37(7):1842-1850

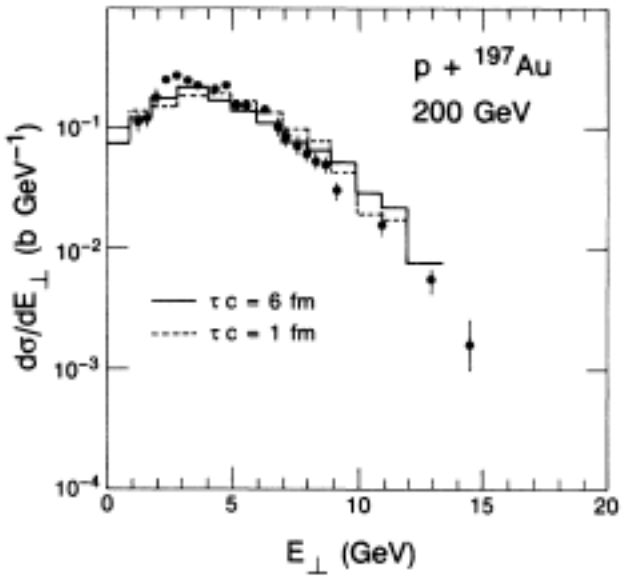

FIG. 8. Transverse-energy distributions $d\sigma/dE_\perp$ for protons interacting on Au nuclei. The calculations given by histograms are compared to data (points) from the NA35 Collaboration[2] measured in the rapidity range $2.2 \leq \eta \leq 3.8$. The Monte Carlo results are presented for two different values of the formation-time parameter τ.

Transverse-energy distributions in p-Au collisions were also measured by the NA35 Collaboration at the CERN Super Proton Synchrotron. This experiment is sensitive for laboratory rapidities 2.2<y <3.8. In this rapidity range we do not expect significant changes of the $d\sigma/dE$ distributions with the τ parameter. In Fig. 8 we find indeed a good agreement of the model for τc =1 fm as well as for τc =6 fm with the data. It is not possible to determine the τ parameter from this experiment. The model agrees well with the data.

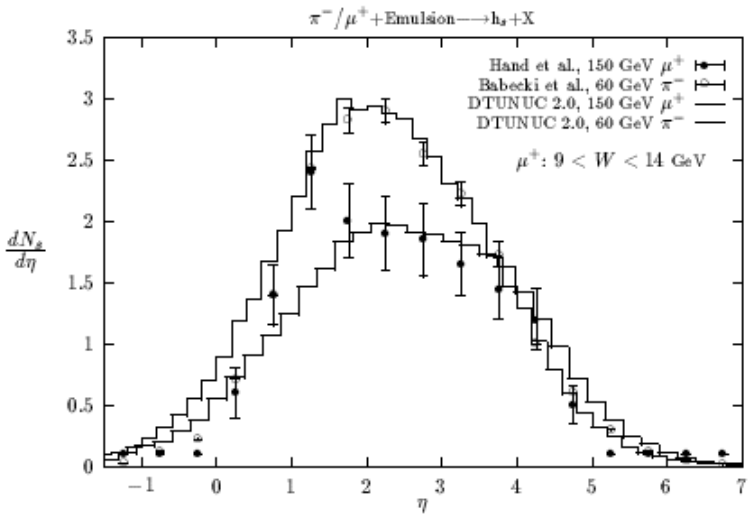

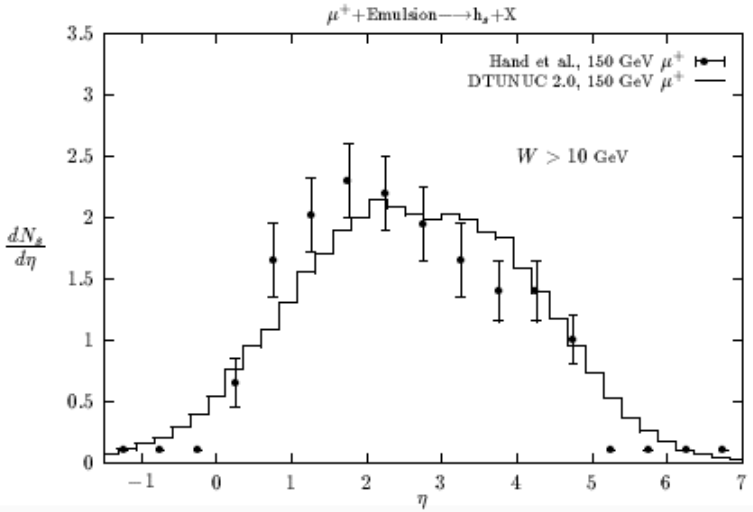

Fig.13

Pseudorapidity distributions of shower particles (β > 0.7) from muon-emulsion interactions at 150 GeV .

In a) the photon-nucleon c.m. energy range is restricted to 9 < W < 14 GeV. In addition, the pseudorapidity distribution of charged hadrons from pion-emulsion interactions at 60 GeV is plotted and compared to data. In b) the results for W > 10 GeV are given. In both distributions
only events with $N_h > 3$ are included.

Photoproduction off nuclei and pointlike photon interactions: cross section and nuclear shadowing:

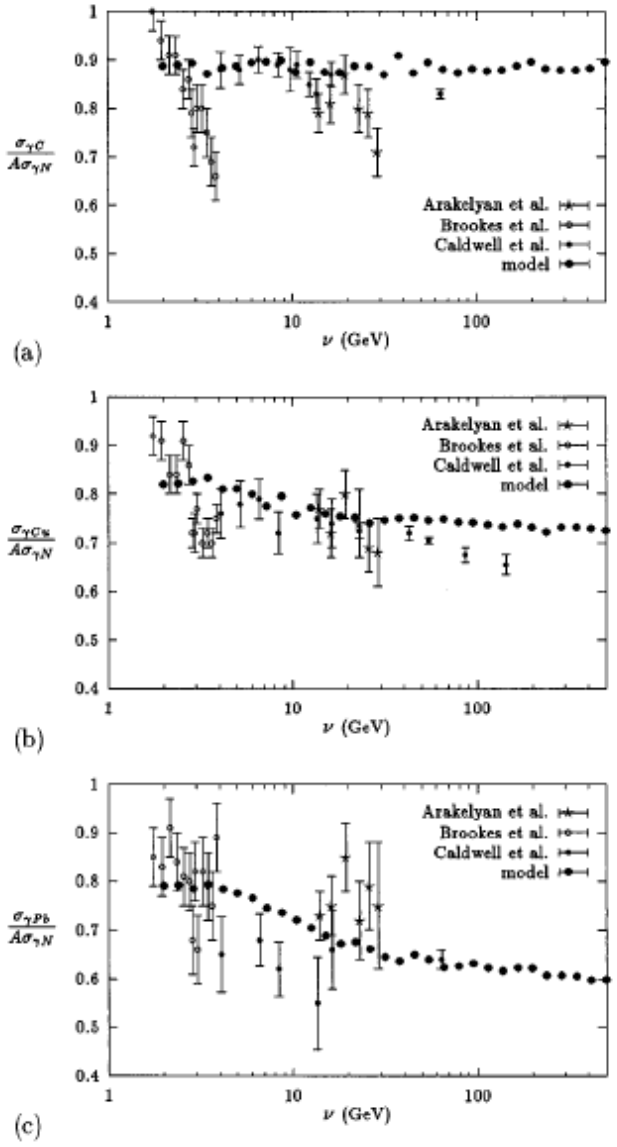

Per-nucleon ratios of real photon-carbon (a), -copper (b), and -lead (c) cross sections to photon-nucleon cross sections

The agreement is reasonable. However, there are considerable uncertainties within the measurements as well as differences between the results obtained in different experiments which make it difficult to draw further conclusions from this comparison.

Arakelyan et al.	Real photon beam with energy range 12-30 GeV
Brookes et al.	photon beam over the energy range 1.7-4 GeV
Caldwell et al.	Energy 3.7-18.3 GeV

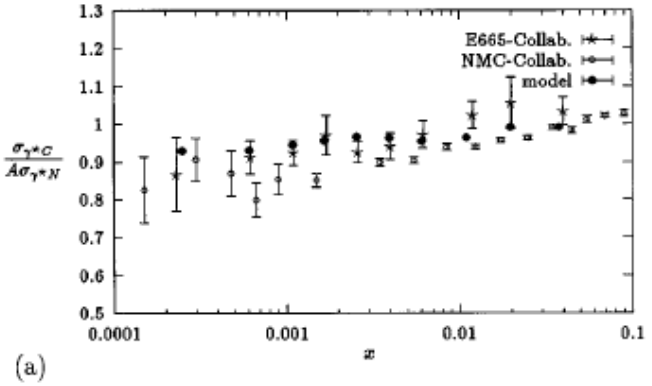

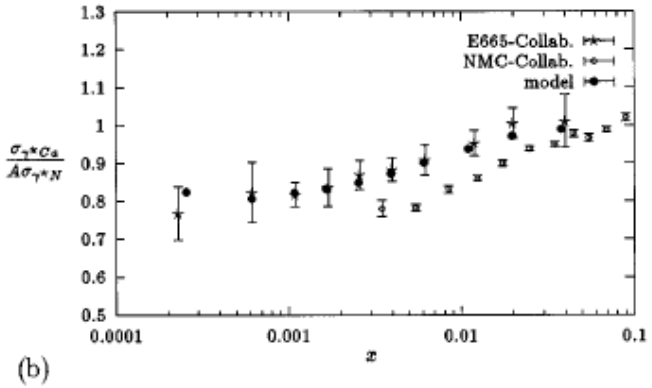

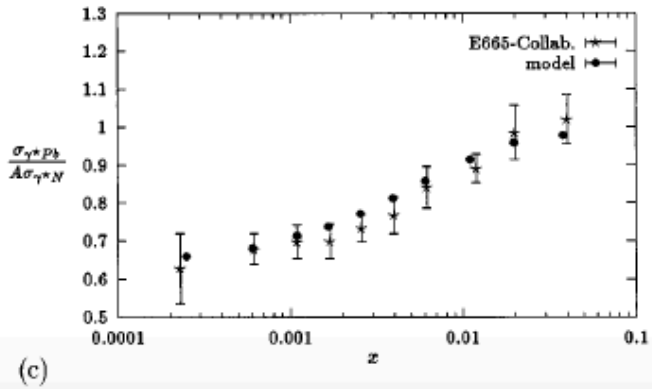

The dependence of the per-nucleon ratios of photoncarbon (a), -calcium (b), and -lead (c) cross sections to photonnucleon cross sections on the Bjorken-x is compared to data of the E665- and NMC-Collaborations.

E665 using 470 GeV/c muons
NMC (New Muon Collaboration) using 200 GeV/c muons

The calculations for the three target nuclei carbon, calcium, and lead are in reasonable agreement with the E665 data but overestimate the NMC data slightly.

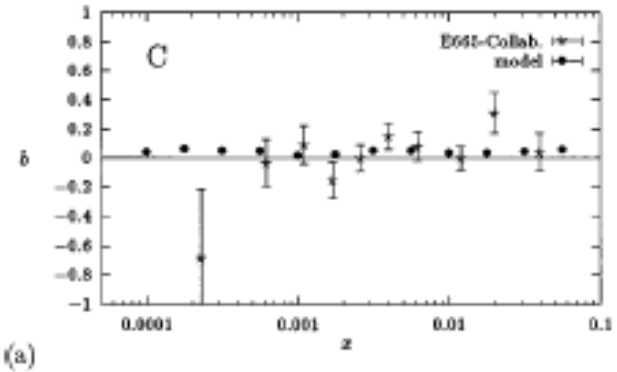

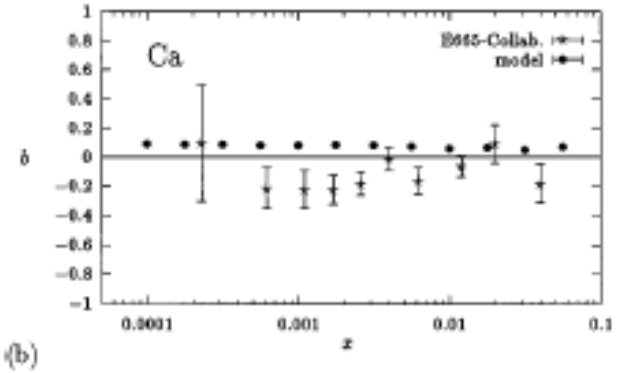

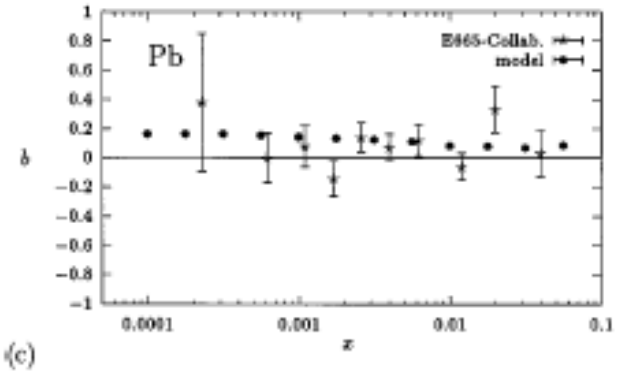

The muon beam momentum： 470 GeV/c

In order to study the Q2 dependence of the cross section ratios at fixed values of x we parametrize them as

$$R^A = \frac{\sigma_{\gamma * A}}{A\sigma_{\gamma * N}} = \mathrm{a} + \mathrm{b} log_{10}(Q^2/GeV^2)$$

the slope b as function of x, again for carbon, calcium, and lead targets, together with E665 measurements.

The results are consistent with the experimental observations, i.e., with a weak Q2 dependence of the shadowing effect within the considered x range.